Deficiency of rds/peripherin causes photoreceptor death in mouse models of digenic and dominant retinitis pigmentosa

Wojciech Kedzierski*, Steven Nusinowitz†, David Birch‡§, Geoff Clarke¶‖, Roderick R. McInnes¶‖, Dean Bok†‡§, and Gabriel H. Travis†¶‖**

*Department of Pharmacology, University of Texas Southwestern Medical Center, Dallas, TX 75390; †Jules Stein Eye Institute, ‡Department of Neurobiology, and ¶Department of Biological Chemistry, University of California School of Medicine, Los Angeles, CA 90095; §Retina Foundation of the Southwest, Dallas, TX 75231; ‖Programs in Developmental Biology and Genetics, Hospital for Sick Children, and Department of Molecular and Medical Genetics, University of Toronto, Toronto, ON, Canada M5C 1X8

Edited by Thaddeus P. Dryja, Harvard Medical School, Boston, MA, and approved May 14, 2001 (received for review March 13, 2001)

Retinitis pigmentosa (RP) is a group of inherited blinding diseases caused by mutations in multiple genes including *RDS*. *RDS* encodes rds/peripherin (rds), a 36-kDa glycoprotein in the rims of rod and cone outer-segment (OS) discs. Rom1 is related to rds with similar membrane topology and the identical distribution in OS. In contrast to *RDS*, no mutations in *ROM1* alone have been associated with retinal disease. However, an unusual digenic form of RP has been described. Affected individuals in several families were doubly heterozygous for a mutation in *RDS* causing a leucine 185 to proline substitution in rds (L185P) and a null mutation in *ROM1*. Neither mutation alone caused clinical abnormalities. Here, we generated transgenic/knockout mice that duplicate the amino acid substitutions and predicted levels of rds and rom1 in patients with *RDS*-mediated digenic and dominant RP. Photoreceptor degeneration in the mouse model of digenic RP was faster than in the wild-type and monogenic controls by histological, electroretinographic, and biochemical analysis. We observed a positive correlation between the rate of photoreceptor loss and the extent of OS disorganization in mice of several genotypes. Photoreceptor degeneration in *RDS*-mediated RP appears to be caused by a simple deficiency of rds and rom1. The critical threshold for the combined abundance of rds and rom1 is ≈60% of wild type. Below this value, the extent of OS disorganization results in clinically significant photoreceptor degeneration.

Retinitis pigmentosa (RP) is a family of inherited retinal diseases characterized by progressive night blindness and loss of peripheral vision (1). Pathologically, RP is associated with degeneration of rod photoreceptors. Heterozygous mutations in the *RDS* gene are a common cause of autosomal dominant RP (2, 3). An example is the *RDS* P216L-allele (4). *RDS* encodes rds/peripherin (rds), a 36-kDa glycoprotein in the rims of rod and cone outer-segment (OS) discs (5, 6). These stacked membranous structures are the sites of photon-capture and reactions of visual transduction. Rom1 is a related disk-rim protein with 37% overall identity and similar membrane topology to rds (7). Mice homozygous for a knockout mutation in the *rom1* gene displayed mild OS dysplasia (8), in contrast to complete absence of OS in *rds*−/− mice (9–11). Unlike *RDS*, no mutations in the *ROM1* gene alone have been convincingly associated with human retinal disease (12, 13). However, an unusual digenic form of RP has been described. Affected individuals in four pedigrees were doubly heterozygous for a mutation in *RDS* causing a leucine 185 to proline substitution in rds (L185P) and a second presumptive null mutation in the unlinked *ROM1* gene (13, 14). Neither mutation alone caused significant abnormalities.

The phenotype in *rds*−/− mutant mice (9, 10) indicates a critical role for rds in the formation of OS. Expression of a chimeric protein in transgenic mice on an *rds*−/− genetic-background established that rds is 2.5-fold more abundant than rom1, and that the rds–rom1 interaction involves the large, intradiscal D2 loop (15). In the current study, we sought to address three questions concerning the biochemical etiology of *RDS*-mediated retinal degeneration. First, can the clinical observation of digenic RP in humans be corroborated in an animal model? Second, how do the pathogenic L185P and P216L D2-loop substitutions affect the abundance of rds? Third, what is the relationship between OS disorganization and photoreceptor degeneration in the different mutant *RDS* alleles? To address these questions, we generated complex transgenic/mutant mice in which both the specific substitutions and levels of rds and rom1 closely matched those predicted for the corresponding human diseases.

Materials and Methods

Generation of Transgenic Mice. We assembled a DNA construct containing a rhodopsin promoter upstream of the mouse rds coding region. We introduced a T to C transition into codon 185, resulting in L185P. The construct was otherwise identical to a previously described transgene encoding normal rds (16). Fertilized oocytes of hybrid strain B6 × DBA mice were microinjected with this construct. Of several L185P lines generated, line 1708 was selected for study based on its level of expression. P216L- and S231A-transgenic mice were generated as described (17, 18). The L185P, P216L, and S231A transgenes were crossed onto *rds*+/−, *rds*−/− (9, 10), *rom1*+/−, and *rom1*−/− (8) mutant backgrounds. Mice were analyzed for presence of the transgenes as described (17). Mice were maintained on a 12-hour light/dark cycle (25–30 lx). For all studies except electroretinogram (ERG) analysis, animals were killed between 4 and 6 h after light-onset.

Nuclease Protection Analysis of Retinal RNAs. Total RNA was extracted from individual eyecups and hybridized to ^{32}P-labeled cRNA probes of 1,041 nt for *rds* or 687 nt for *rom1*. After digestion with S1 nuclease, protected fragments were separated by electrophoresis through an 8% polyacrylamide gel containing 8 M urea. Bands were quantitated with reference to a standard curve of *in vitro*-transcribed sense *rds*-mRNA on a Molecular Dynamics model 425F PhosphorImager.

This paper was submitted directly (Track II) to the PNAS office.

Abbreviations: ERG, electroretinogram; L185P, leucine 185 to proline substitution in rds; ONL, outer nuclear layer; OS, outer segment; rds, rds/peripherin protein; Rmp_3, a-wave maximal response by ERG; RP, retinitis pigmentosa; rds C-term Ab and rom1 C-term Ab, antisera against residues 296–346 from the carboxy terminus of rds and residues 296–351 from the carboxy terminus of rom1.

**To whom reprint requests should be addressed at: Jules Stein Eye Institute, 100 Stein Plaza, University of California School of Medicine, Los Angeles, CA 90095. E-mail: travis@jsei.ucla.edu.

The publication costs of this article were defrayed in part by page charge payment. This article must therefore be hereby marked "*advertisement*" in accordance with 18 U.S.C. §1734 solely to indicate this fact.

Table 1. Expected and observed levels of rds and rom1 monomers in mouse retinas

Genotype	rds expected (% w/t)	rds observed (% w/t ± SEM)	rom1 expected (% w/t)	rom1 observed (% w/t ± SEM)
Wild-type	100	(100)	100	(100)
rom1+/−	100	106 ± 4	50	58 ± 2
L185P *rds*+/−	100	62 ± 2	100	103 ± 2
Digenic	100	51 ± 2	50	42 ± 2
rds+/−	50	26 ± 2	100	67 ± 2
P216L *rds*+/−	100	8 ± 1	100	25 ± 3
rom1−/−	100	100 ± 4	0	0
S231A *rds*+/−	50	45 ± 4	100	99 ± 10

Expected levels of rds and rom1 monomers relative to wild-type (w/t) were based on measurements of the respective endogenous and transgenic mRNAs by nuclease protection analysis without considering the effects of reduced protein stability or outer-segment dysplasia. Observed levels of rds and rom1 were obtained by quantitative immunoblotting, as represented in Fig. 5*a*. Values are expressed as an average percent of the wild-type signal on each blot ± SEM. For S231A *rds*+/− mice, contributions of the nonglycosylated protein (lower rds band in Fig. 5*a*) were not included.

Electroretinography. Full-field ERGs were obtained from mice of the genotypes indicated in Fig. 4. After overnight dark-adaptation, mice were anesthetized with ketamine (200 mg/kg) plus xylazine (10 mg/kg) and the pupils were dilated with topical 1.0% atropine sulfate. ERGs were obtained in a Ganzfeld dome, using a gold coil wire overlaid with 1% methylcellulose on the corneal surface, a similar reference electrode in the mouth, and a needle ground-electrode in the tail. A high-intensity flash unit (Novatron, Dallas, TX) provided short-wavelength flashes (Kodak Wratten 47B) at intensities 1 to 3.4 log scot td-sec in 0.3 log unit steps. The leading edge of the a-waves was fit (as an ensemble; ref. 19) by the Lamb and Pugh model for the activation phase of the phototransduction cascade (20). The maximal response (Rmp_3) and the amplification constant (S) were calculated from this model.

Preparation of Samples for Light and Electron Microscopy. Mice were anesthetized with Nembutal (75 mg/kg) and fixed by vascular perfusion for 5 min with 1% formaldehyde and 2% glutaraldehyde in 0.1 M sodium phosphate buffer (pH 7.2). Eyes were removed and immersed in the same fixative overnight at 4°C, then fixed for an additional hour in 1% osmium tetroxide. Tissues were dehydrated and embedded in Araldite 502 (Ted Pella, Redding, CA). Sections (0.5 μm) were cut on glass knives and stained with toluidine blue for light microscopy. Ultrathin sections were cut with a diamond knife and stained with uranium and lead salts for electron microscopy.

Immunoblot Analysis. Antisera against residues 296–346 from the carboxy terminus of rds (rds C-term Ab) and residues 296–351 from the carboxy terminus of rom1 (rom1 C-term Ab) were prepared as described (15). For the quantitative immunoblotting, retinal homogenates were separated by SDS/PAGE and transferred to Immobilon P-SQ (Millipore) in buffer containing 0.05% SDS. After reacting with the primary antibody, blots were labeled by using ^{125}I-protein A (ICN) in a 6-hr incubation at a concentration of 0.1 μCi/ml (1 Ci = 37 GBq). After five 8-min washes, the radioactive bands were visualized and quantitated on a Molecular Dynamics model 425F PhosphorImager. In a control experiment, the radioactive signal was shown to increase linearly with loaded protein up to 4% retina per lane. Quantitation was performed with 2% retina loaded per lane. Radioactive signals for rds and rom1 were determined as a fraction of the wild-type signal on each blot. The data presented in Table 1 represent the averages of these fractions.

Immunoprecipitation Analysis. Before immunoprecipitation, the rom1 C-term Ab was coupled to Affi-Gel Hz beads (Bio-Rad). Dissected retinas from mice of the indicated genotypes were homogenized in Triton buffer (50 mM Tris·HCl, pH 7.5, 100 mM NaCl, 5 mM EDTA, 1% Triton X-100, 0.05% SDS, 2.5% glycerol, and protease inhibitors). Homogenates were cleared by a 2-min spin at 4°C and incubated with the coupled Ab at 4°C for 2 h. Beads were washed and the bound proteins were eluted with 2× sample buffer for immunoblot analysis. Approximately 50% of total rds in each extract was precipitated with the rom1 C-term Ab.

Results

Levels of the *rds* and *rom1* mRNAs in Transgenic Retinas. To determine expression of the *rds* and *rom1* genes, we performed nuclease protection analysis on retinal RNA prepared from mice of the relevant genotypes (Fig. 1). The spontaneous *rds* mutation in mice results from insertion of an extraneous repetitive element into exon 2 (21). Although the disrupted gene is transcribed in *rds*−/− photoreceptors (protected band visible in Fig. 1), no protein product is made (16, 21). Thus, the spontaneous *rds* allele is null. The mRNA product of the L185P transgene in line 1708 mice was present at ≈50% the level of the endogenous transcript by quantitative nuclease-protection analysis (Fig. 1). No mRNA is transcribed from the disrupted gene in *rom1* knockout mice

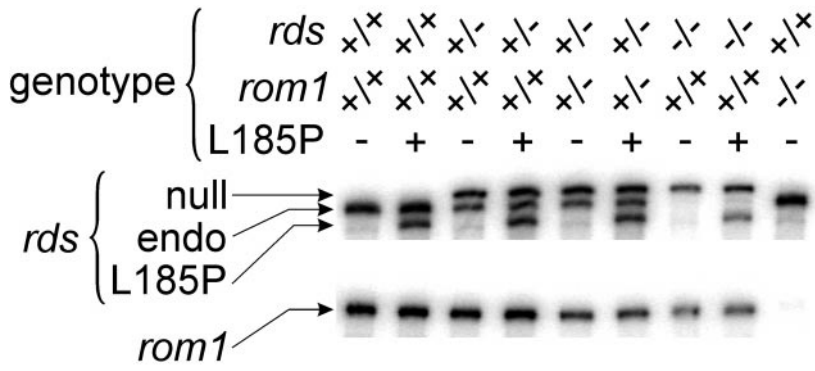

Fig. 1. Nuclease protection analysis of *rds* and *rom1* mRNAs. RNA was prepared from 3-week-old L185P-transgenic and nontransgenic mouse retinas of the indicated genotypes. (*Upper*) The three fragments protected with a 1,041-nt *rds* cRNA-probe: a band of 1,011 nt corresponding to the spontaneous *rds*-mutant mRNA (null), 899 nt corresponding to the normal endogenous *rds* mRNA (endo), and 843 nt corresponding to the mRNA product of the L185P-transgene (L185P). (*Lower*) The single 659-nt band protected by a 687-nt *rom1* cRNA-probe corresponding to the normal *rom1* mRNA (*rom1*).

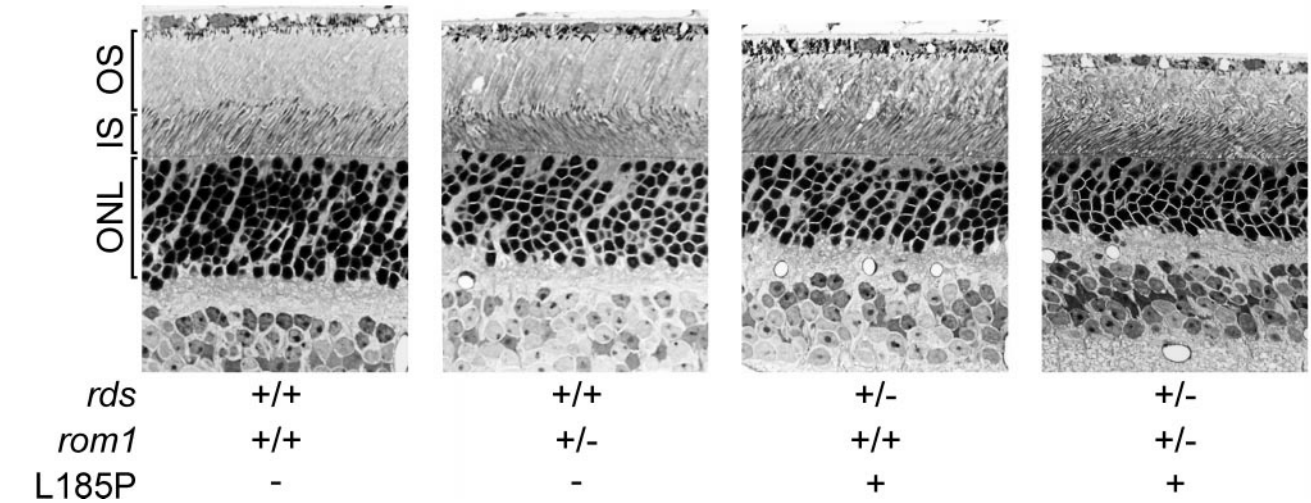

Fig. 2. Light microscopy of mouse retinas. Outer retinas from 9-month-old mice of the indicated genotypes are shown. The OS, inner segment (IS), and ONL are indicated. Note the reduced ONL thickness in L185P *rds*+/− and digenic mice compared with the wild-type control. (×430.)

(ref. 8; Fig. 1). The L185P transgene was crossed onto *rds* (9, 10) and *rom1* (8) mutant backgrounds. Previously, we generated mice with a similar transgene encoding P216L-substituted rds (17). Mice from P216L line 1376 express the transgene in retina at ≈60% the level of the normal endogenous *rds* mRNA (17). We also generated transgenic mice that express an mRNA encoding S231A-substituted (nonglycosylated) rds at ≈80% the level of the normal endogenous *rds* mRNA (18).

Slow Photoreceptor Degeneration in a Mouse Model of Digenic RP. We examined sections of retina from mice of the relevant genotypes by light microscopy. Fig. 2 shows a representative set of light micrographs from 9-month-old mice. The extent of photoreceptor loss can be estimated by observing the thickness of the outer nuclear layer (ONL) in retinal sections. The ONL thickness was reduced in L185P *rds*+/− and digenic compared with wild-type mice (Fig. 2). No difference in ONL thickness was apparent in *rom1*+/− compared with wild-type mice. These data indicate photoreceptor loss in L185P *rds*+/− and digenic mice.

Expression of L185P-Substituted, but Not P216L-Substituted rds Corrects the OS Disorganization in *rds*+/− Retinas. To estimate the degree of OS dysplasia in mice of the different genotypes, we

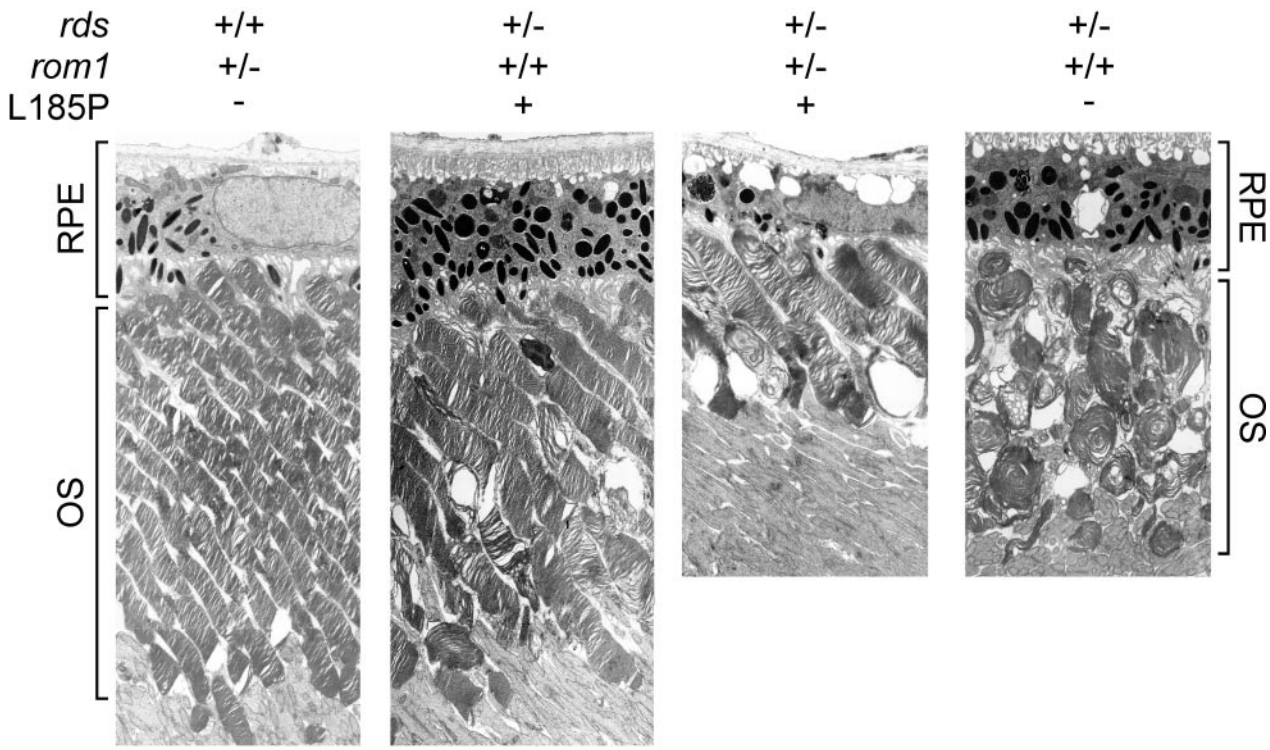

Fig. 3. Electron microscopy of mouse retinas. OS and retinal pigment epithelium (RPE) layers of retinas from 9-month-old mice of the indicated genotypes are shown. Note the shortening and disorganization of OS in the digenic retina. Also note the distortion of OS into whorl structures in the *rds*+/− retina. (×3,000.)

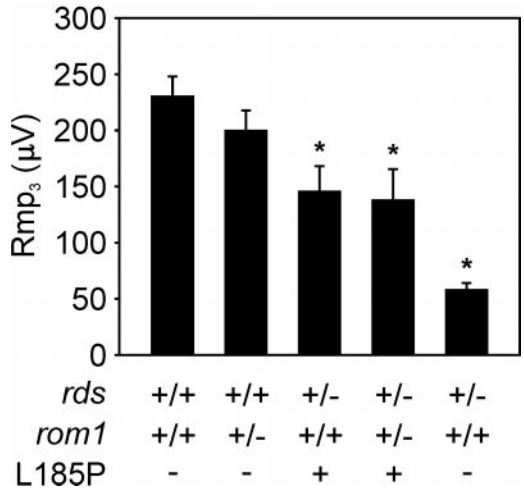

Fig. 4. Electroretinographic analysis. ERGs were performed on five to 7-month-old mice of the genotypes: wild-type ($n = 13$), *rom1*+/− ($n = 11$), L185P *rds*+/− ($n = 3$), digenic ($n = 7$), and nontransgenic *rds*+/− ($n = 8$). Average values of Rmp_3 for mice of the indicated genotypes are plotted in microvolts ($\mu V \pm$ SEM). An asterisk above the data bar denotes a significant difference from the wild-type value of Rmp_3 (Student's *t* test; $P < 0.01$).

examined retinas of 9-month-old mice by electron microscopy. The morphology of OS in *rom1*+/− mice was indistinguishable from wild type (Fig. 3). Mild dysplasia was noted in L185P-transgenic *rds*+/− mice, with slight shortening and widening of OS and misalignment of discs. The dysplasia was more severe in the digenic mice, with profound shortening of OS and disorganization of discs. As described (22), gross disorganization of OS was seen in *rds*+/− mice with replacement of the discs by large whorl structures. This dysplasia was not corrected by expression of P216L-substituted rds, as shown (17).

Reduced Retinal Photoresponse in *rds*-Mutant and Digenic Mice. To probe the function of photoreceptors *in vivo*, we analyzed wild-type and mutant mice by electroretinography. ERG records the electrical response of the retina to a light flash on the corneal surface. The initial a-wave results from photoreceptor hyperpolarization. We computed the a-wave maximal amplitude (Rmp_3; ref. 23) for each animal studied. A reduction in Rmp_3 is associated with loss of functional discs due to abnormal development of OS or degeneration of photoreceptors (19). The average Rmp_3 values obtained for mice of the indicated genotypes at approximately 6 months are shown in Fig. 4. Rmp_3 was significantly reduced in L185P *rds*+/− monogenic and L185P *rds*+/−, *rom1*+/− (digenic) compared with wild-type mice. Rmp_3 was further reduced in nontransgenic *rds*+/− mice. The amplification constants (S) was within normal limits for all mice tested.

Levels of Normal and Substituted rds and rom1 Proteins in Mice of Different Genotypes. To determine the levels of rds and rom1, we analyzed retinal homogenates from transgenic and nontransgenic mice on several genetic backgrounds by quantitative immunoblotting. Mice were analyzed at 3 weeks of age, before the onset of significant photoreceptor death in any mutants. Immunoblots were performed in quintuplicate for rds and quadruplicate for rom1, using the rds and rom1 C-term Abs (15) and ^{125}I-labeled protein A for detection. The results of a representative experiment are presented in Fig. 5*a*. Table 1 shows the levels of rds and rom1 in retinas from mice of each genotype expressed as a fraction of the level in wild-type retinas. The level of rds in *rds*+/− retinas was 26% that of wild-type retina, significantly less than the 50% predicted by levels of the endogenous mRNA in wild-type and *rds*+/− retinas (Fig. 1). The S231A substitution eliminates the single conserved site of *N*-glycosylation in rds, resulting in a protein of reduced molecular mass but normal function (18). Use of the S231A *rds*−/− background permitted immunoblot quantitation of other rds forms. Expression of S231A-substituted rds in transgenic mice completely rescued the *rds*+/− phenotype of disorganized OS (18). Accordingly, the level of endogenous (glycosylated) rds in *rds*+/− mice expressing the S231A transgene was close to the predicted value (45% vs. 50%). The level of total rds was significantly higher in L185P-transgenic *rds*+/− (62% of wild type) compared with nontransgenic *rds*+/− retinas, consistent with synthesis of additional L185P-substituted rds. Because OS were intact in these mice (Fig. 3), L185P-substituted rds must be transported to the OS where it must function normally. In contrast, expression of P216L-substituted rds in *rds*+/− retinas

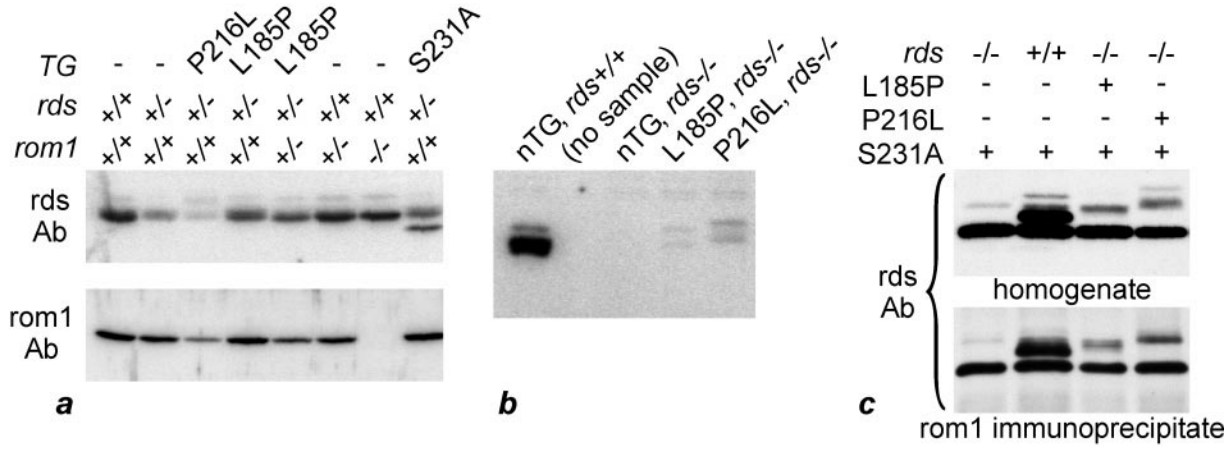

Fig. 5. Immunoblot analysis of rds and rom1 in mouse retinas. (*a*) Quantitative immunoblotting of homogenates from rds P216L-, L185P-, and S231A-transgenic retinas of the indicated genotypes at *rds* and *rom1*. Blots were incubated with antibodies against the rds C-term (rds) or rom1 C-term (rom1) antibodies. Note the reduced levels of rds in nontransgenic *rds*+/− and P216L *rds*+/− homogenates. Also note the lower mass of nonglycosylated, S231A-substituted rds. (*b*) Levels of rds in nontransgenic (nTG), L185P-, and P216L-transgenic *rds*−/− retinas. All mice were wild-type at *rom1*. Note the dramatically reduced levels of substituted rds in retinas from L185P- and P216L-transgenic mice. (*c*) Coimmunoprecipitation of normal, L185P-, P216L-, and S231A-substituted rds with rom1. The genotypes at *rds* are indicated, all mice were wild-type at *rom1*. The band of lower molecular mass in all lanes is S231A-substituted rds. Note the similar protein abundance profiles in the starting homogenates and rom1-immunoprecipitated samples.

resulted in significantly reduced total rds (8% of wild type). OS in P216L-transgenic *rds*+/− retinas were considerably more dysplastic than nontransgenic *rds*+/− retinas, as shown (17). Finally, although rom1 was undetectable, rds was present at approximately normal levels in *rds*+/+, *rom1*−/− retinas (Fig. 5*a*), consistent with the relatively normal OS in mice of this genotype (8).

L185P- and P216L-Substituted rds Are Dramatically Reduced in *rds*−/− Retinas. To what extent does the function of L185P-substituted rds depend on the presence of normal rds? To address this question, we moved the L185P and P216L transgenes onto an *rds*−/− null genetic background. Immunoblot analysis showed dramatically reduced L185P- and P216L-substituted rds in *rds*−/− compared with wild-type retinas (Fig. 5*b*). These data indicate that in the absence of normal rds, the L185P- and P216L-substituted proteins are either unstable or not transported to OS. Consistent with these biochemical results, neither P216L- nor L185P-substituted rds rescued the phenotype of absent OS in *rds*−/− mice (data not shown). The low levels of both substituted proteins indicate that neither are accumulating within the endoplasmic reticulum (ER).

L185P- and P216L-Substituted rds Efficiently Coprecipitate with rom1. Covalent homodimers of rds normally interact with rom1 homodimers to form a higher-order noncovalent complex in the disk rim (15, 24–27). To test the interaction of rom1 with L185P-substituted rds, we performed immunoprecipitation analysis with the rom1 C-term Ab on retinal homogenates from doubly transgenic mice that express S231A-substituted plus L185P- or P216L-substituted rds on a wild-type or *rds*−/− genetic background (Fig. 5*c*). The rom1 C-term Ab does not cross react with rds (15). Both L185P- and P216L-substituted rds coprecipitated with similar efficiency to normal rds. These data indicate that the L185P and P216L D2-loop substitutions do not disturb the interaction of rds with rom1.

Discussion

Digenic Inheritance of Retinal Degeneration in an Animal Model. Digenic inheritance of RP was originally reported in patients doubly heterozygous for a mutation in *RDS* causing an L185P substitution plus an early frame-shift mutation in *ROM1* (13, 14). To verify digenic inheritance of RP, we placed a transgene that expresses L185P-substituted rds at ≈50% the level of endogenous rds on an *rds*+/−, *rom1*+/− double heterozygous genetic background. The ERG results were in general agreement between the mouse and human models of digenic RP (14). In the mice, reduced ERG amplitudes were correlated with degeneration of photoreceptors by light microscopy. Together, these data validate digenic inheritance of RP in humans.

Photoreceptor Degeneration Is Correlated with Abnormal Development of OS. We observed a good correlation between the extent of OS disorganization and the degree of photoreceptor degeneration. A progressive increase in the severity of both phenotypic parameters was observed in the series: (*i*) *rom1*+/−; (*ii*) L185P *rds*+/−; (*iii*) digenic; (*iv*) *rds*+/− (22); (*v*) P216L *rds*+/− (17); and (*vi*) *rds*−/− (9, 10). The mechanism of photoreceptor degeneration in *rds* mutants is unknown. Because no accumulation of substituted rds was observed in L185P- and P216L-transgenic *rds*−/− mice, ER stress can be ruled out. Oxygen toxicity is another possibility. According to this mechanism, reduced cation influx through cGMP-gated channels causes reduced activity of Na^+/K^+-ATPases and hence reduced uptake of O_2 by mitochondria. The resulting increased pO_2 causes oxidative damage to photoreceptors (28). The observed congruence between the extent of OS dysplasia and the rate of photoreceptor death here and in other studies (17, 22) supports this hypothesis. Mutations in the gene for rhodopsin are also responsible for a subset of autosomal dominant RP. The ultrastructural effects of several RP-associated mutations in the rhodopsin gene have been studied in transgenic mice, including the heterozygous-null, P347S, P23H, V20G, and P27L alleles (29–32). Shortening and disorganization of OS was observed in all cases. Thus, the principle of photoreceptor degeneration due to OS dysplasia may extend to mutations in multiple genes.

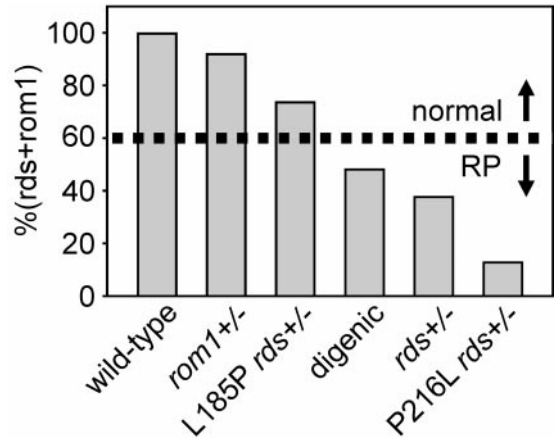

Fig. 6. Abundance of rds plus rom1 in mouse models of human *RDS*-mediated retinal degenerations. The levels of rds plus rom1 as a fraction of wild-type [%(rds + rom1)] in mice of the indicated genotypes were calculated from the data in Table 1, assuming a 2.5:1 abundance ratio of rds to rom1 (15, 27). Minimal photoreceptor degeneration was seen in monogenic (*rom1*+/− and L185P-transgenic *rds*+/−) mice. Humans of the corresponding genotypes were asymptomatic (14). Slow photoreceptor degeneration was seen in L185P-transgenic *rds*+/−, *rom1*+/− (digenic) mice. Humans of the corresponding genotype had slowly progressive digenic RP (14). Slightly faster retinal degeneration was seen in *rds*+/− mice and in humans of the corresponding genotype (33–38). Finally, severe photoreceptor degeneration was seen in P216L-transgenic *rds*+/− mice. Humans heterozygous for an *RDS* P216L mutation have dominant RP (4). Thus, the level of rds + rom1 required to prevent disease is ≈60% of wild type. When the combined abundance of these proteins falls below this value (indicated by the dashed line), photoreceptor degeneration becomes clinically recognizable as RP.

Covalent Homodimers of L185P- and P216L-Substituted rds Are Unstable. The mRNA products of the L185P and P216L transgenes were present at ≈50% the level of the normal endogenous *rds* mRNA (ref. 17; Fig. 1). Thus, approximately equal levels of the mutant and normal *rds* mRNAs are present in L185P- and P216L-transgenic *rds*+/− retinas. If monomers of normal and substituted rds dimerized stochastically, and if each dimer form were equally stable, the distribution of normal–normal, normal–substituted, and substituted–substituted dimers should be 1:2:1. However, the capacity of L185P-substituted rds to rescue the *rds* phenotype was strongly dependent on the presence of normal rds. Also, the level of rds was close to wild type in L185P-transgenic *rds*+/− retinas, but undetectable in both L185P- and P216L-transgenic *rds*−/− retinas (Fig. 5*b*). These data suggest that covalent homodimers of L185P- and P216L-substituted rds do not form or are unstable. Consistent with these observations, it was shown (24) that expression of L185P-substituted rds in cultured cell membranes resulted in an impaired rds homointeraction, but normal interactions between rds and rom1. Given the absence of L185P–L185P homodimers, the maximum possible level of rds in L185P-transgenic *rds*+/− mice is 75% of wild type. The actual level observed was 62% (Table 1). Because OS are relatively intact in these mice (Fig. 3), we conclude that heterodimers of normal and L185P-substituted rds must also form functional complexes. Coimmunoprecipitation of L185P-

substituted rds with a rom1 antibody (Fig. 5*c*) supports this conclusion. In contrast, the level of rds in P216L-transgenic *rds*+/− mice was only 8% of wild type. This suggests that with P216L, both normal–substituted and substituted–substituted dimers are unstable. A possible explanation for the profound OS disorganization and photoreceptor degeneration in P216L-transgenic mice (17), and the severity of RP in humans with a P216L mutation in *RDS* (4), is depletion of the normal rds protein due to degradation of normal–P216L heterodimers.

The L185P and P216L Mutations Cause a Deficiency of rds. The abundance of rds is ≈2.5-fold that of rom1 (15, 27). This value, combined with the data in Table 1, permits us to calculate the total abundance of rds plus rom1 (rds + rom1) as a percent of wild type in mice of each genotype according to the equation:

$$\%(\text{rds} + \text{rom1}) = \frac{2.5(\%\text{rds}) + (\%\text{rom1})}{3.5}$$

If we assume that rds and rom1 are functionally equivalent, we can compare rds + rom1 to the phenotype in several forms of *rds*-mediated retinal degeneration (Fig. 6). Mice were analyzed by quantitative immunoblotting at 3 weeks, before the onset of photoreceptor degeneration. The level of rds + rom1 in nontransgenic *rom1*+/− heterozygotes is 92% of wild type. We observed virtually no photoreceptor degeneration in these mice by histologic or ERG analysis. Consistently, no mutations in rom1 alone have been associated with any human disease (13). L185P *rds*+/− mice, with a level of rds + rom1 at 74%, exhibited mild photoreceptor degeneration. Humans of the corresponding genotype were asymptomatic, but showed slightly reduced ERG amplitudes and prolonged implicit times (14). Very mild photoreceptor degeneration was also observed in *rom1*−/− knockout mice (8), with an estimated level of rds + rom1 at 71% of wild type. We observed significant photoreceptor degeneration and OS dysplasia in digenic mice. The estimated level of rds + rom1 in these animals is 48%. Humans of the corresponding genotype have slowly progressive RP (14). Slightly more severe photoreceptor degeneration and OS dysplasia were seen in nontransgenic *rds*+/− mice, with a level of rds + rom1 at 38%. Slowly progressive RP in patients heterozygous for presumptive *RDS* null alleles have been described in several reports (33–38). Finally, rapid photoreceptor degeneration and profound OS dysplasia were observed in P216L-transgenic *rds*+/− mice (17). The level of rds + rom1 in these mice was 13%. This substitution causes dominant RP in humans (4). Together, these results suggest a critical threshold for the level of rds + rom1 in the range between 48% and 71% (average = 60%) of wild type. At levels below this approximate value, the extent of OS disorganization results in clinically significant photoreceptor degeneration. One prediction of this model is that transgenic overexpression of rom1 may rescue the *rds*+/− phenotype. In conclusion, these studies show that rds protein deficiency is a common etiologic factor in at least three forms of *RDS*-mediated retinal degeneration.

We gratefully acknowledge Walid Moghrabi for generating rds and rom1 C-term Abs, and Marsha Lloyd, Mark Pennesi, and Roxana Radu for their outstanding technical assistance. This work was supported by grants from the National Eye Institute (EY08043, EY00444, and EY00331), the Foundations Fighting Blindness of United States and Canada, and the Canadian Genetic Disease Network. R.M. is an International Research Scholar of the Howard Hughes Medical Institute. D.B. is the Dolly Green Professor of Ophthalmology at the University of California, Los Angeles, and a Research to Prevent Blindness Senior Scientific Investigator. G.H.T. is the Charles Kenneth Feldman Professor of Ophthalmology at the University of California, Los Angeles.

1. Heckenlively, J. R. (1988) in *Retinitis Pigmentosa*, ed. Heckenlively, J. R. (Lippincott, Philadelphia), pp. 221–252.
2. Keen, T. J. & Inglehearn, C. F. (1996) *Hum. Mutat.* **8,** 297–303.
3. Kohl, S., Giddings, I., Besch, D., Apfelstedt-Sylla, E., Zrenner, E. & Wissinger, B. (1998) *Acta Anatomica* **162,** 75–84.
4. Kajiwara, K., Hahn, L. B., Mukai, S., Travis, G. H., Berson, E. L. & Dryja, T. P. (1991) *Nature (London)* **354,** 480–483.
5. Connell, G., Bascom, R., Molday, L., Reid, D., McInnes, R. R. & Molday, R. S. (1991) *Proc. Natl. Acad. Sci. USA* **88,** 723–726.
6. Travis, G. H., Sutcliffe, J. G. & Bok, D. (1991) *Neuron* **6,** 61–70.
7. Bascom, R. A., Manara, S., Collins, L., Molday, R. S., Kalnins, V. I. & McInnes, R. R. (1992) *Neuron* **8,** 1171–1184.
8. Clarke, G., Goldberg, A. F. X., Vidgen, D., Collins, L., Ploder, L., Schwarz, L., Molday, L. L., Rossant, J., Szel, A., Molday, R. S., Birch, D. G. & McInnes, R. R. (2000) *Nat. Genet.* **25,** 67–73.
9. van Nie, R., Ivanyi, D. & Demant, P. (1978) *Tissue Antigens* **12,** 106–108.
10. Sanyal, S. & Jansen, H. G. (1981) *Neurosci. Lett.* **21,** 23–26.
11. Travis, G. H., Brennan, M. B., Danielson, P. E., Kozak, C. A. & Sutcliffe, J. G. (1989) *Nature (London)* **338,** 70–73.
12. Bascom, R. A., Liu, L., Heckenlively, J. R., Stone, E. M. & McInnes, R. R. (1995) *Hum. Mol. Genet.* **4,** 1895–1902.
13. Dryja, T. P., Hahn, L. B., Kajiwara, K. & Berson, E. L. (1997) *Invest. Ophthalmol. Visual Sci.* **38,** 1972–1982.
14. Kajiwara, K., Berson, E. L. & Dryja, T. P. (1994) *Science* **264,** 1604–1608.
15. Kedzierski, W., Weng, J. & Travis, G. H. (1999) *J. Biol. Chem.* **274,** 29181–29187.
16. Travis, G. H., Groshan, K. R., Lloyd, M. & Bok, D. (1992) *Neuron* **9,** 113–119.
17. Kedzierski, W., Lloyd, M., Birch, D. G., Bok, D. & Travis, G. H. (1997) *Invest. Ophthalmol. Visual Sci.* **38,** 498–509.
18. Kedzierski, W., Bok, D. & Travis, G. H. (1999) *J. Neurochem.* **72,** 430–438.
19. Hood, D. C. & Birch, D. G. (1994) *Invest. Ophthalmol. Visual Sci.* **35,** 2948–2961.
20. Lamb, T. D. & Pugh, E. N., Jr. (1992) *J. Physiol.* **449,** 719–758.
21. Ma, J., Norton, J. C., Allen, A. C., Burns, J. B., Hasel, K. W., Burns, J. L., Sutcliffe, J. G. & Travis, G. H. (1995) *Genomics* **28,** 212–219.
22. Hawkins, R. K., Jansen, H. G. & Sanyal, S. (1985) *Exp. Eye Res.* **41,** 701–720.
23. Hood, D. C. & Birch, D. G. (1993) *Visual Neurosci.* **10,** 857–871.
24. Goldberg, A. F. & Molday, R. S. (1996) *Proc. Natl. Acad. Sci. USA* **93,** 13726–13730.
25. Moritz, O. L. & Molday, R. S. (1996) *Invest. Ophthalmol. Visual Sci.* **37,** 352–362.
26. Goldberg, A. F. X., Loewen, J. R. & Molday, R. S. (1998) *Biochemistry* **37,** 680–685.
27. Loewen, C. J. R. & Molday, R. S. (2000) *J. Biol. Chem.* **275,** 5370–5378.
28. Travis, G. (1998) *Am. J. Hum. Genet.* **62,** 503–508.
29. Humphries, M. M., Rancourt, D., Farrar, G. J., Kenna, P., Hazel, M., Bush, R. A., Sieving, P. A., Sheils, D. M., McNally, N., Creighton, P., *et al.* (1997) *Nat. Genet.* **15,** 216–219.
30. Naash, M. I., Hollyfield, J. G., al-Ubaidi, M. R. & Baehr, W. (1993) *Proc. Natl. Acad. Sci. USA* **90,** 5499–5503.
31. Li, T., Snyder, W., Olsson, J. & Dryja, T. (1996) *Proc. Natl. Acad. Sci. USA* **93,** 14176–14181.
32. Liu, X. R., Wu, T. H., Stowe, S., Matsushita, A., Arikawa, K., Naash, M. I. & Williams, D. S. (1997) *J. Cell Sci.* **110,** 2589–2597.
33. Kajiwara, K., Sandberg, M. A., Berson, E. L. & Dryja, T. P. (1993) *Nat. Genet.* **3,** 208–212.
34. Meins, M., Gruning, G., Blankenagel, A., Krastel, H., Reck, B., Fuchs, S., Schwinger, E. & Gal, A. (1993) *Hum. Mol. Genet.* **2,** 2181–2182.
35. Wells, J., Wroblewski, J., Keen, J., Inglehearn, C., Jubb, C., Eckstein, A., Jay, M., Arden, G., Bhattacharya, S., Fitzke, F., *et al.* (1993) *Nat. Genet.* **3,** 213–218.
36. Lam, B. L., Vandenburgh, K., Sheffield, V. C. & Stone, E. M. (1995) *Am. J. Ophthalmol.* **119,** 65–71.
37. Apfelstedt-Sylla, E., Theischen, M., Ruther, K., Wedemann, H., Gal, A. & Zrenner, E. (1995) *Br. J. Ophthalmol.* **79,** 28–34.
38. Jacobson, S. G., Cideciyan, A. V., Kemp, C. M., Sheffield, V. C. & Stone, E. M. (1996) *Invest. Ophthalmol. Visual Sci.* **37,** 1662–1674.